



PAGE

Form Approved
OMB No. 0704-0188

Public reporting burden for this collection of information is estimated to average 1 hour per response, including the time for reviewing instructions, searching existing data sources, gathering and maintaining the data needed, and completing and reviewing the collection of information. Send comments regarding this burden estimate or any other aspect of this collection of information, including suggestions for reducing this burden, to Washington Headquarters Services, Directorate for Information Operations and Reports, 1215 Jefferson Davis Highway, Suite 1204, Arlington, VA 22202-4302, and to the Office of Management and Budget, Paperwork Reduction Project (0704-0188), Washington, DC 20503.

1. AGENCY USE ONLY (Leave blank)	2. REPORT DATE February 1994	3. REPORT TYPE AND DATES COVERED Professional Paper
----------------------------------	---------------------------------	--

4. TITLE AND SUBTITLE THE PERFORMANCE OF ADAPTIVE EQUALIZATION FOR DIGITAL COMMUNICATION SYSTEMS CORRUPTED BY INTERFERENCE	5. FUNDING NUMBERS PR: CG17 PE: 0602234N WU: DN303156
6. AUTHOR(S) R. C. North, R. A. Axford, and J. R. Zeidler	

7. PERFORMING ORGANIZATION NAME(S) AND ADDRESS(ES) Naval Command, Control and Ocean Surveillance Center (NCCOSC) RDT&E Division San Diego, CA 92152-5001	8. PERFORMING ORGANIZATION 94-08836
---	---

9. SPONSORING/MONITORING AGENCY NAME(S) AND ADDRESS(ES) Office of Naval Research 800 North Quincy Street Arlington, VA 22217	
---	--

**DTIC
SELECTED
MAR 21 1994**

11. SUPPLEMENTARY NOTES

12a. DISTRIBUTION/AVAILABILITY STATEMENT Approved for public release; distribution is unlimited.	12b. DISTRIBUTION CODE
---	------------------------

13. ABSTRACT (Maximum 200 words)

This paper analyzes the effects of interference on the steady-state performance of several popular adaptive equalization algorithms. It is shown that adaptive equalizers based on the linear equalizer structure have a built-in capability to reject narrowband interference, however performance deteriorates as the bandwidth of the interference increases. The existence of a time-varying misadjustment component in the adaptive equalizer weight vector is shown to affect the interference cancellation properties. In addition, simultaneous multipath propagation and interference is investigated. These effects on the performance of the adaptive linear equalizer are especially important to applications where intentional or unintentional interferers may be encountered.

Accession For	By	Availability Codes	Avail and/or Special
<input checked="" type="checkbox"/> NTIS <input type="checkbox"/> CRA&J <input type="checkbox"/> DTIC TAB <input type="checkbox"/> Unannounced <input type="checkbox"/> Justification	Distribution /		
			Dist A-1 20

Published in *ASILOMAR Conference on Signals, Systems and Computers*, October 1993, 6 pages.

14. SUBJECT TERMS adaptive equalization mobile communications spatial-temporal processing	15. NUMBER OF PAGES
	16. PRICE CODE
17. SECURITY CLASSIFICATION OF REPORT UNCLASSIFIED	18. SECURITY CLASSIFICATION OF THIS PAGE UNCLASSIFIED
19. SECURITY CLASSIFICATION OF ABSTRACT UNCLASSIFIED	20. LIMITATION OF ABSTRACT SAME AS REPORT

94 3 18 082

UNCLASSIFIED

21a. NAME OF RESPONSIBLE INDIVIDUAL R. C. North	21b. TELEPHONE (include Area Code) (619) 553-4323	21c. OFFICE SYMBOL Code 824

The Performance of Adaptive Equalization for Digital Communication Systems Corrupted by Interference

Richard C. North, Roy A. Axford, and James R. Zeidler
 NCCOSC RDT&E Division
 San Diego, CA 92152-7304

Abstract

This paper analyzes the effects of interference on the steady-state performance of several popular adaptive equalization algorithms. It is shown that adaptive equalizers based on the linear equalizer structure have a built-in capability to reject narrowband interference, however performance deteriorates as the bandwidth of the interference increases. The existence of a time-varying misadjustment component in the adaptive equalizer weight vector is shown to affect the interference cancellation properties. In addition, simultaneous multipath propagation and interference is investigated. These effects on the performance of the adaptive linear equalizer are especially important to applications where intentional or unintentional interferers may be encountered.

I. Introduction

Modern digital communication systems typically employ modulation formats like *M*-PSK or *M*-QAM to increase spectral efficiency (eg. bits/sec/Hz) of the transmitted signal. Successful use of these spectrally efficient modulation formats requires the receiver to have a greater capability to: (1) compensate for distortion introduced by the channel, transmitter, and receiver, (2) cancel interference, and (3) provide for matched filtering. Adaptive equalization is a single channel technique which is frequently used in receivers to compensate for linear distortion (eg. intersymbol interference (ISI)) introduced by the channel and transmit/receive filters. It can be particularly useful when the channel distortion is not known precisely or is time-varying. In this paper, we examine the ability of the adaptive linear equalizer (AEQ) to reject additive interference.

Previous work has shown that the adaptive linear predictor (ALP) can be effective in cancelling (or enhancing) narrowband interference [1]-[8]. The ALP forms a narrowband notch centered at the interferer frequency by exploiting the sample-to-sample correlation in the narrowband interferer. Broadband interference was considered for the ALP in [9] and [10]. In [10], it was shown that the ALP performance degrades rapidly as the bandwidth of the interferer increases. As the bandwidth of the interference increases, the sample-to-sample correlation decreases and the predictability of the interference decreases. Similar results for the AEQ are presented in this paper.

The analysis technique used in this paper will be to decompose the output of the adaptive linear equalizer into a Wiener filter (WF) term and a Misadjustment filter (MF) term. This is an established technique which offers insight into the dynamics of the adaptation process [3]. For the

conditions investigated in this text, the second-order statistics of the output will be approximately the sum of the second-order statistics of the output of the WF and the output of the MF. The MF will be further separated into a random component and a time-varying component. The random MF is generated by the gradient estimation noise and will be quantified here as being uncorrelated with a resulting white spectrum. The time-varying MF is generated by periodic terms in the filter input, $x(k)$, and will be sample-to-sample correlated giving a colored spectrum. It is the time-varying MF that gives rise to the "spectral broadening" in the ALP [4] and the "notch broadening" in the adaptive noise canceller (ANC) [12]-[15]. It will be shown in this paper that the performance of the ALP and the AEQ are dependent on their respective time-varying MFs. Under certain conditions, the time-varying MF is shown to enhance the CW cancelling capabilities of the AEQ.

Only *T*-spaced 2-sided adaptive linear equalizers will be presented. Future work will include fractionally spaced AEQs with and without decision feedback. While numerous fast algorithms exist for adapting the equalizer's weights, this paper will consider the Least Mean Square (LMS) algorithm [16], the stabilized Fast Transversal Filter (FTF) RLS algorithm [17] and the RLS Lattice algorithm with directly updated coefficients (DUPL) [18].

The rest of this paper is organized as follows: Section II provides a brief description of the signal and interference models and the AEQ structure. Section III analyzes the performance of the AEQ with CW interference and no multipath. It is shown that the WF of the AEQ is a constant multiple of the WF of the ALP. However, the differences in performance are significant and linked to the difference in their MFs. Ideal bandpass Gaussian noise is presented in Section IV as an interferer whose bandwidth is easily controlled. Performance of the AEQ is shown to degrade rapidly as the bandwidth of the interferer increases. Section IV also shows some simulation results of the AEQ faced with both a multipath channel and interference. Performance degradation is found to be a function of the severity of the multipath as might be expected.

II. Preliminaries

A. Signal Model

The complex baseband representation of the received signal can be written as,

$$x(t) = h(t) * s(t) + i(t) + n(t) \quad (1)$$

where $h(t)$, $s(t)$, $i(t)$, and $n(t)$ are the complex baseband channel impulse response, transmitted signal, interference signal, and additive noise respectively. This paper will consider the case of a time-invariant two-path channel, $h(t) = h_1\delta(t) + h_2\delta(t - \tau_c)$, where τ_c is the channel delay

spread. The complex baseband channel can be related to the real bandpass channel by $h_1 = H_1$ and $h_2 = H_2 e^{-j2\pi f_c \tau_d}$ where H_1 and H_2 are the direct path and multipath tap-gains of the real bandpass channel and f_c is the carrier frequency [19]. For digital communication, the complex baseband transmitted signal is described by, $s(t) = \sqrt{2S} \sum_k s_k P_T(t - kT)$, where S is the average transmitted signal power, $\{s_k\}$ represents a sequence of symbols transmitted at the symbol rate of $R = 1/T$ symbols per second and $P_T(t)$ is the baseband pulse shape.

The autocorrelation of Eq. (1) can be written as [19],

$$\begin{aligned} \phi_{x,x}(\tau) &\equiv \frac{1}{2} E[x(t) x^*(t - \tau)] \\ &= \phi_{h_1,h_1}(\tau) + \phi_{i,i}(\tau) + \phi_{n,n}(\tau) \end{aligned} \quad (2)$$

where it has been assumed that the components of $x(k)$ are mutually uncorrelated. Using the two-path channel model, it can be shown that,

$$\begin{aligned} \phi_{h_1,h_2}(\tau) &= (h_1 h_2^*) \phi_{s,s}(\tau + \tau_d) + (|h_1|^2 + |h_2|^2) \phi_{s,s}(\tau) \\ &\quad + (h_1^* h_2) \phi_{s,s}(\tau - \tau_d) \end{aligned} \quad (3)$$

where for $P_T(t) = 1$ in the interval $[0, T]$ and 0 elsewhere,

$$\phi_{s,s}(\tau) = \begin{cases} S \left(1 - \frac{|\tau|}{T}\right) & -T \leq \tau \leq T \\ 0 & \text{otherwise} \end{cases} \quad (4)$$

Two types of interference are analyzed in this paper. The first is CW interference given by, $i(t) = \sqrt{2I} e^{j(2\pi f_\Delta t + \phi)}$, where I , f_Δ , ϕ are the power, carrier offset frequency, and phase of the interference respectively. The autocorrelation of the CW interference is,

$$\phi_{i,i}(\tau) = I e^{+j2\pi f_\Delta \tau} \quad (5)$$

The second type of interference is bandpass white Gaussian noise with power spectra defined by,

$$PSD_x(f) = \begin{cases} N_B & f_\Delta - \frac{B}{2} \leq f \leq f_\Delta + \frac{B}{2} \\ 0 & \text{otherwise} \end{cases} \quad (6)$$

Its autocorrelation can be computed by taking the inverse Fourier transform of Eq. (6) giving,

$$\phi_{i,i}(\tau) = N_B B \left(\frac{\sin(\pi B \tau)}{\pi B \tau} \right) e^{+j2\pi f_\Delta \tau} \quad (7)$$

This interference model encompasses both narrowband and broadband interference with a single parameter, the bandwidth B . For very small but finite B , Eq. (7) reduces to Eq. (5) where $I = N_B B$ is equal to the total baseband interferer power.

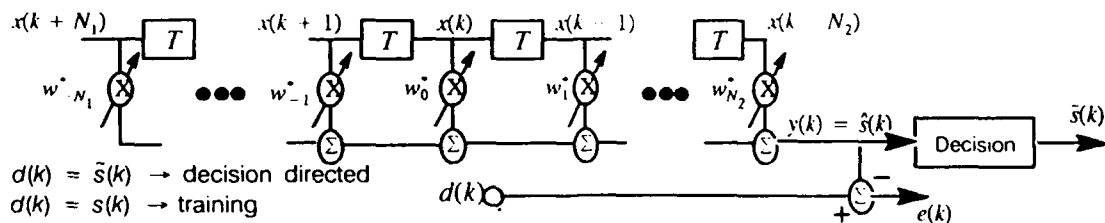


Fig. 1: 2-sided T-Spaced Adaptive Linear Equalizer.

Finally, the additive noise is assumed to come from a white Gaussian process with power spectral density $PSD_n(f) = N_0$ for all frequencies. Its auto-correlation function is $\phi_{n,n}(\tau) = \sigma_n^2 \delta(\tau) = N_0 \delta(\tau)$.

B. Adaptive Linear Equalizer Structure

Fig. 1 illustrates the 2-sided T -spaced AEQ where T is the symbol duration. The ideal equalizer will extract the transmitted signal, $s(k)$ [for notational convenience $s(kT)$ will be written as $s(k)$], from the received data described by Eq. (1) at each instant in time. In this paper, it will be assumed that the receiver has perfect symbol synchronization and that no carrier offset exists. The filter output and the filter error output can be written as, $y(k) = w^H(k) x(k)$ and $e(k) = d(k) - y(k)$ where $w(k) = [w_{-N_1}(k), \dots, w_0(k), \dots, w_{N_2}(k)]^T$, $x(k) = [x(k + N_1), \dots, x(k), \dots, x(k - N_2)]^T$, $d(k)$ is the desired signal (also called the primary signal), and H indicates Hermitian transpose.

The AEQ is typically employed in the receiver of a digital communication system with the (ideal) task of (1) correcting for intersymbol interference (ISI), (2) cancelling interference, and (3) providing matched filtering. The AEQ requires a priori information about the transmitted signal, usually in the form of a training sequence. After the symbol error rate decreases below about 0.01, symbol decisions can be used as the desired signal. It will be assumed that the combination of training and decision-direction results in only correct symbols used for the desired signal.

Note that Fig. 1 can be easily modified to form a 2-sided T -spaced ALP (also called an adaptive whitening filter or an adaptive line enhancer with unit decorrelation delay) by setting $w_0 = 0$ and $d(k) = x(k)$. With this configuration, the ALP will first estimate the interference with the filter output, $y(k)$, and then subtract this from the received signal, $x(k)$, resulting in an estimate of the transmitted signal at the filter error output, $e(k)$. (Note that another functionally equivalent configuration of the ALP is $w_0 = -1$ and $d(k) = 0$, which results in the filter output estimating the negative of the transmitted signal.) The ALP has the advantage of not requiring a priori information about the transmitted signal. It can be effective in cancelling narrowband interference (see for instance [7],[8]) but was shown in [10] to degrade system performance when *no interference* is present. It is introduced here because of its similarities with the AEQ, both structurally and operationally, although the AEQ will always out perform the ALP for $SNR > 0$ dB.

III. Performance with CW Interference

The adaptive linear equalizer weights can be decomposed into a WF and a MF,

$$w(k) = w^{opt} + w^{mis}(k) \quad (8)$$

The WF is a time-invariant solution that can be found by solving the normal equation. It is the optimum solution in the sense of minimizing the mean squared error (MSE), $E[|e(k)|^2]$. Once the WF is found, the MF can be found from Eq. (8). Each component of the filter output can then be analyzed separately since $y(k) = (w^{opt})^H x(k) + (w^{mis}(k))^H x(k)$. If $w^{mis}(k)$ is approximately uncorrelated with $x(k)$, and $E[w^{mis}(k)] = 0$ (or equivalently when $E[w(k)] = w^{opt}$), then we may write the power spectrum of the filter output as,

$$P_y(\omega) = P_y^{opt}(\omega) + P_y^{mis}(\omega) \quad (9)$$

Even though the existence of a time-varying MF could result in a time dependence of $E[w^{mis}(k)]$, insight will be gained by plotting the terms in Eq. (9) separately.

A. Wiener Filter

The AEQ will have a Wiener component of the weight vector as long as the cross-correlation between the filter input, $x(k)$, and the desired signal, $d(k) = s(k)$, satisfies $\phi_{xs}(l) \neq 0$ for $l = -N_1, \dots, N_2$. The Wiener component can be found from the normal equation,

$$\sum_{n=-N_1}^{N_2} w_n^{opt} \phi_{xx}^*(l-n) = \phi_{xs}^*(l) \text{ for } l = -N_1, \dots, N_2. \text{ This can}$$

be solved by the method of undetermined coefficients for the CW interferer case (as was done in [1] for the 1-sided ALP and in [7] for the 2-sided ALP filter) by letting $w_n^{opt} = A_n e^{j\omega n}$ for $\omega_\Delta = 2\pi f_\Delta/f$, where f_Δ/f is the offset frequency normalized to the sampling frequency. Solving for A_n it can be shown that,

$$A_0 = \frac{1}{1 + \frac{\sigma_n^2}{S} + \frac{I}{S} \left[1 - \frac{1}{1 + \frac{S + \sigma_n^2}{I(N_1 + N_2)}} \right]} \quad (10)$$

$$A = A_n = - \frac{A_0}{(N_1 + N_2) + \left(\frac{S + \sigma_n^2}{I} \right)}$$

for $n = -N_1, \dots, -1, 1, \dots, N_2$. The frequency response of the WF can be found from $w^{opt}(\omega) = \sum_{n=-N_1}^{N_2} w_n^{opt} e^{-j\omega n}$ for $N = N_1 = N_2$ to be,

$$w^{opt}(\omega) = A_0 \left[1 - \frac{2}{2N + \left(\frac{S + \sigma_n^2}{I} \right)} \cos\left(\frac{\Delta\omega}{2}(N+1)\right) \frac{\sin\left(\frac{\Delta\omega}{2}N\right)}{\sin\left(\frac{\Delta\omega}{2}\right)} \right] \quad (11)$$

where $\Delta\omega = \omega - \omega_\Delta$ and A_0 given by Eq. (10). Eq. (11) describes the frequency response of the AEQ WF between the filter input, $x(k)$, and the filter output, $y(k)$. From Eq. (11) it can be seen that the WF of the AEQ creates a notch filter centered at the center frequency of the interferer. As the filter length increases, the bandwidth of the notch decreases and the depth of the notch increases.

It is interesting that the Wiener weights of the 2-sided AEQ derived above are a constant multiple (A_0) of the Wiener weights of the 2-sided ALP derived in [7] (which is also identical in form to the Wiener weights of the 1-sided ALP derived in [1],[2],[5]). This implies that one might expect the performance of the AEQ filter to be similar to that of the ALP filter. However, it will be shown below that the performance of the AEQ is superior to that of the ALP for SNR > 0dB due to the differences in their MF.

Given the Wiener weight solution, the average power at the output of the Wiener filter can be found from the autocorrelation of the output of the WF for zero lag,

$$\phi_{yy}^{opt}(0) = A_0^2 (S + \sigma_n^2) \left[1 + \frac{N_1 + N_2}{(N_1 + N_2 + \frac{S + \sigma_n^2}{I})^2} \right] + A_0^2 I \left(1 - \frac{N_1 + N_2}{N_1 + N_2 + \frac{S + \sigma_n^2}{I}} \right)^2 \quad (12)$$

The first term in Eq. (12) is the WF output power due to the two broadband components while the second term is the WF output power due to the CW interferer. Note that for a finite length filter, the residual CW power is nonzero.

B. Misadjustment Filter

The characteristics of the MF depend on the weight update equation used in the AEQ. The MF will be further separated into a random MF and a time-varying MF. The weights of the random MF (time-varying MF) will be assumed to be uncorrelated (correlated) from sample-to-sample.

The time-varying MF exists because the CW interferer is present in the filter input, $x(k)$, but not in the desired signal, $d(k)$. A similar condition is reported in [13] and [15] for the ANC. The time constants of the time-varying MF are equal to time constants of the mean of the weight vector, $E[w(k)]$, which are for the LMS filter [12],

$$\tau_{LMS}^i \approx \frac{1}{2\mu\lambda_i} \frac{1}{f_s} \text{ (sec)} \quad (13)$$

for $i = 1, 2, \dots, N_{filter}$ and where $N_{filter} = N_1 + N_2 + 1$ and μ is the LMS step-size. It can be shown that the eigenvalues of the input correlation matrix are $\lambda_1 = I N_{filter} + S + \sigma_n^2$, $\lambda_i = S + \sigma_n^2$ for $i = 2, \dots, N_{filter}$. An equivalent expression for the time constant in either the FTF or the DUPL algorithm is [11],

$$\tau_{RLS} \approx \frac{1}{1-W} \frac{1}{f_s} \text{ (sec)} \quad (14)$$

where W is the exponential weighting parameter. It is important to recognize that τ_{RLS} is independent of the power in the components of the input signal and independent of the filter length unlike τ_{LMS} .

To estimate the magnitude of the misadjustment component, consider the approximate expression for the output power of the MF [12],

$$\phi_{yy}^{mis}(0) \approx \mu \zeta_{min} N_{filter} (S + I + \sigma_n^2) \quad (15)$$

for ζ_{min} equal to the minimum MSE. An exact analysis of $\phi_{yy}^{mis}(k)$, similar to that presented in [4] for the 1-sided ALP, is beyond the scope of this paper.

C. Discussion and Simulations

Figs. 2-5 show simulation results for the AEQ with high SNR and a QPSK signal. Probability of symbol error, P_s , is found from Monte Carlo simulations after convergence. From Fig. 2 it can be seen that both the LMS AEQ and the DUPL AEQ work very well in cancelling the CW interference. The stabilized form of the FTF AEQ [17] sometimes becomes unstable as the SIR ratio decreases. This is presumably due to the large condition number of the input correlation matrix. A closer look at the symbol errors in the FTF AEQ shows that they occur in bursts when the algorithm automatically reinitializes. Figs. 3 and 4 show that the performance of the LMS AEQ (and the DUPL AEQ in Fig. 6) is equal to or better than the WF.

It is interesting to note in Fig. 4 that the measurable 3dB bandwidth in the filter output is smaller for a larger LMS step-size. The reason for this is found in Fig. 5 where the output spectrum of the filter output is separated into its WF and MF components. The AEQ is seen to use its time-varying MF to fill the notch created in the filter output spectrum by the finite length WF. This reduces the filter error output power below that of just the WF. As the step-size is reduced the MF spectral peak in Fig. 5 becomes more narrow. This suggests that as the time constant increases, the time-varying MF is unable to adjust fast enough to compensate for the notched data (ISI) created by the WF.

While the DUPL AEQ follows the same trend as the SNR is increased to 10dB, the situation changes for the LMS AEQ as illustrated in Fig. 6. For the LMS AEQ, $\zeta_{min} \approx \sigma_n^2$, thus the magnitude of the MF (Eq. (15)) is much larger than in the previous case. The ability of the AEQ to estimate the transmitted signal depends on both the magnitude of the MF and on the time constant associated with the weight vector given by Eqs. (13) and (14).

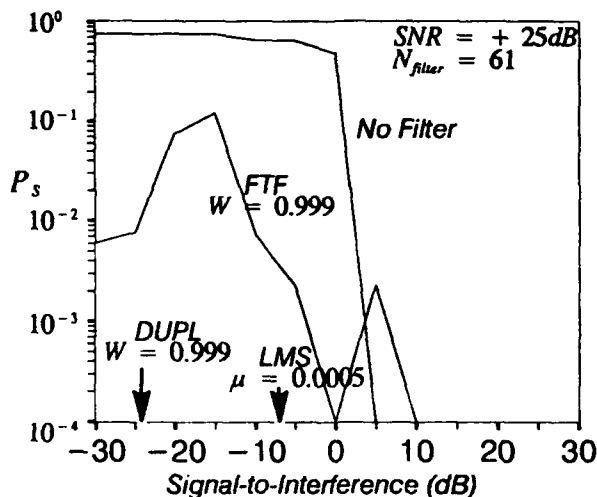


Fig. 2: P_s for LMS, FTF, and DUPL AEQ as a function of CW Interferer power.

Recall that this section showed that for the case of CW interference and no multipath the WF of the AEQ was within a constant multiple of the WF of the ALP. However,

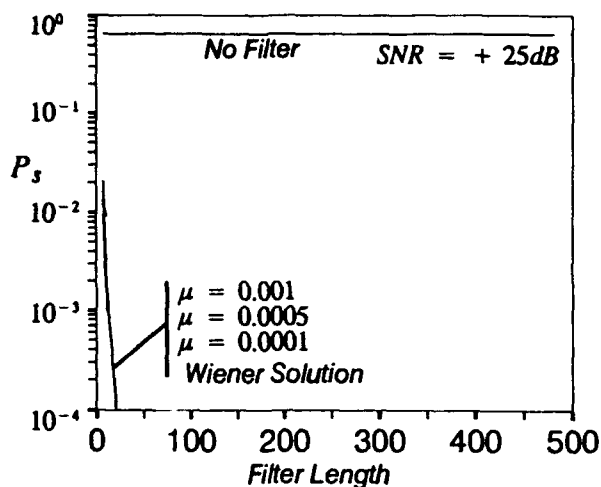


Fig. 3: P_s for LMS AEQ with CW Interferer SIR = -10dB, SNR=+25dB.

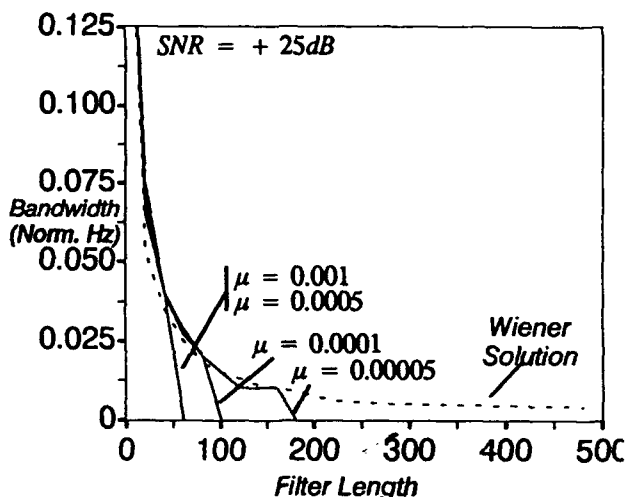


Fig. 4: Notch Bandwidth in the Filter Output of the LMS AEQ created by a CW Interferer SIR = -10dB.

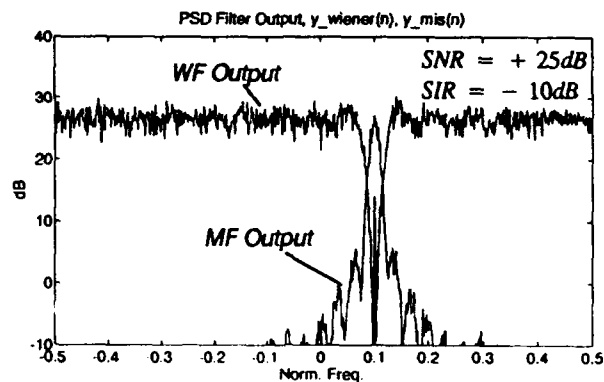


Fig. 5: Output Spectrum of LMS AEQ with CW Interferer $\mu = 0.001$, $N_{filter} = 31$.

Figs. 7-9 show quite clearly that the performance of the AEQ is superior to that of the ALP for high SNR. This is due to the difference in the magnitude of the MF and due to a difference in the operation of the time-varying MF. For the

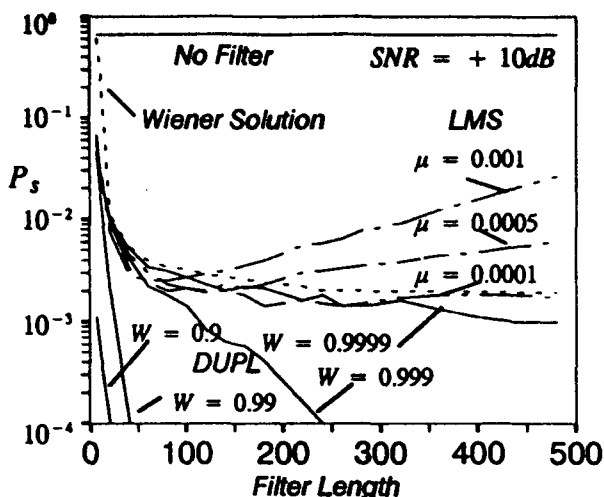


Fig. 6: P_s for LMS & DUPL AEQ with CW Interferer SIR = -10dB, SNR = +10dB.

AEQ. $\zeta_{min} \approx \sigma_n^2$, but for the ALP $\zeta_{min} \approx S$, thus the magnitude of the MF in the ALP is 25 dB greater than that in the AEQ. Fig. 8 shows that the reason the ALP performance degrades with filter length is that the time-varying MF is creating a notch in the error output, destroying $s(k)$. The 3dB bandwidth of the notches match the expression, $BW \approx 1/(\pi \tau_{min})$, (plotted in dashed lines in Fig. 8) which was shown in [15] to be created by the time-varying MF. Fig. 9 illustrates that if the power in the MF was larger (as is the case in Fig. 8 for large filter lengths), the time-varying MF would enhance the depth and the width of the notch created in the error output by the finite length WF. Thus, by generating a spectrally broadened estimate of the interference the ALP can cancel the interference but also cancels the communication signal and as a result the probability of symbol error degrades.

Thus, under a high SNR condition, the time-varying MF improves the AEQ filter performance over that of the WF alone while it degrades the ALP filter performance over that of the WF alone. However, the performance of the AEQ was shown to be dependent on the SNR since the SNR in part determines the magnitude of the MF.

IV. Performance with Broadband Interference and Multipath

For the case of broadband interference and/or multipath, the WF can be found by using Eqs. (2), (3), and (7) to solve the normal equation numerically. This analysis shows that the WF must compromise between rejecting the interference and correcting for multipath induced ISI. To reject broadband interference, the WF forms a spectral notch of bandwidth B centered at the interference offset frequency. To cancel ISI, the WF forms a spectral peak to compensate for the spectral null in the multipath channel. The MF is found from simulation results to fill the notch created by the WF in a similar fashion as that previously discussed for CW interference.

Figs. 10 and 11 illustrate the effect of broadband inter-

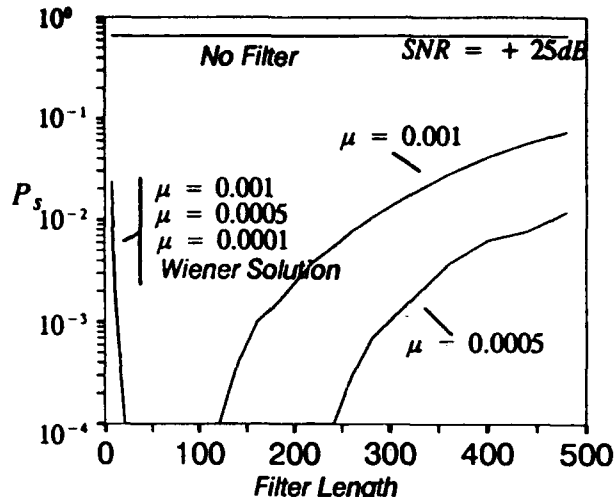


Fig. 7: P_s for LMS ALP with CW Interferer SIR = -10dB, SNR = +25dB.

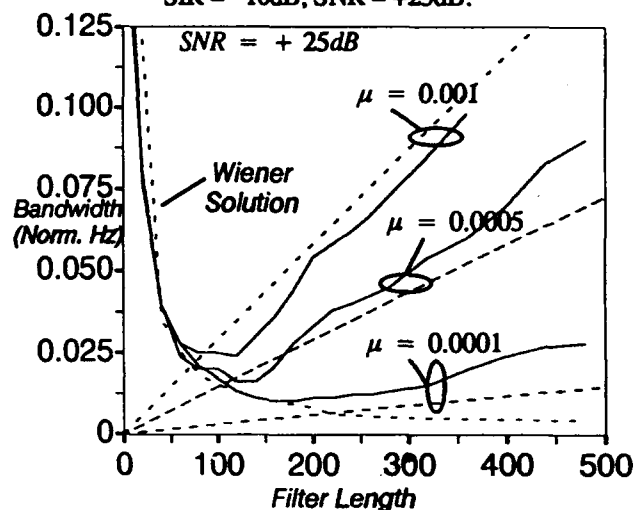


Fig. 8: Notch Bandwidth in the Error Output of the LMS ALP created by a CW Interferer SIR=-10dB.

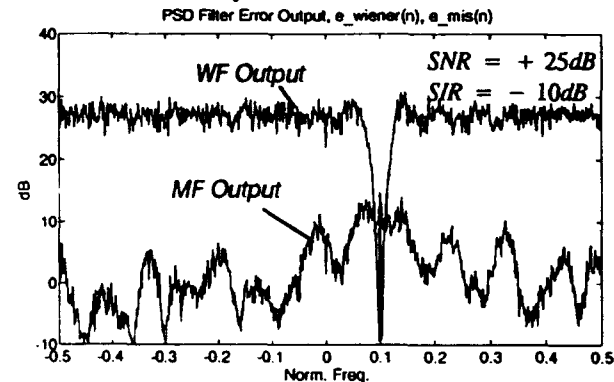


Fig. 9: Output Spectrum of LMS ALP with CW Interferer $\mu = 0.001$, $N_{filter} = 31$. interference with multipath (dashed lines) ($h_1 = 1.0$, $h_2 = 0.9 \angle -30^\circ$) and without multipath (solid lines). From the figures it is clear that the AEQ with $N_{filter} = 61$ is extremely sensitive to the bandwidth and to the power of the broadband interferer. The performance of the AEQ with

$B > 0$ degrades more rapidly as $|h_2| \rightarrow |h_1|$. Note that the DUPL AEQ is less sensitive to multipath than the LMS AEQ presumably because the RLS algorithm is approximately independent of the conditioning of the input correlation matrix. The FTF AEQ which displays stable operation for broadband interference without multipath, shows increasing instability as $|h_2| \rightarrow |h_1|$.

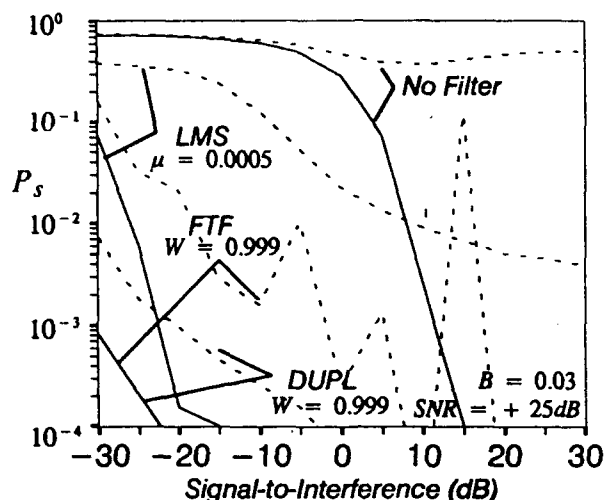


Fig. 10: P_s for LMS, FTF, and DUPL AEQ with $B=0.03$ Broadband Interferer and Multipath.

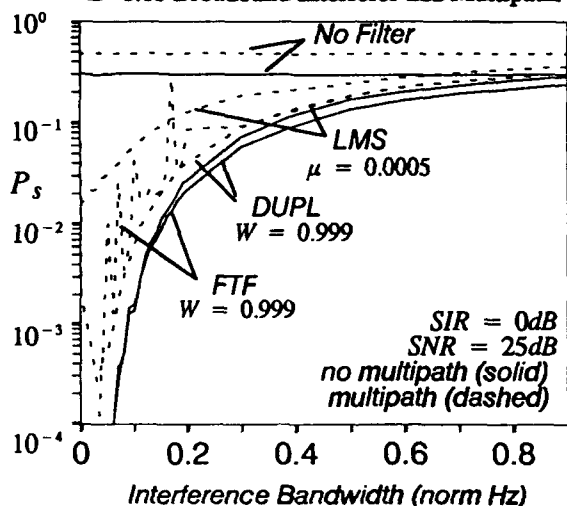


Fig. 11: P_s for LMS, FTF, and DUPL AEQ with Broadband Interferer $SIR = 0dB$ and Multipath.

V. Conclusion

This paper has analyzed the effects of interference on the LMS, FTF and DUPL AEQs. It was shown that the AEQ rejects interference by creating a notch in the frequency response of the WF, but that the time-varying MF can under certain conditions fill the notch (compensate for WF generated ISI) thereby improving performance over that of the WF alone. In addition, it was shown that for simultaneous multipath and interference, the performance of the AEQ is based on a compromise between compensating for ISI and rejecting interference. Simulation results suggest that for applications where intentional or unintentional interferes may exist,

techniques other than adaptive equalization alone, such as multi-channel processing, should be investigated.

References

- [1] J. Zeidler, E. Satorius, D. Chabies, and H. Wexler, "Adaptive Enhancement of Multiple Sinusoids in Uncorrelated Noise," *IEEE Trans. on ASSP*, vol. ASSP-26, no. 3, pp. 240-254, June, 1978.
- [2] J. Treichler, "Transient and Convergent Behavior of the Adaptive Line Enhancer," *IEEE Trans. on ASSP*, vol. ASSP-27, no. 1, pp. 53-62, Feb., 1979.
- [3] J. Rickard and J. Zeidler, "Second-Order Output Statistics of the Adaptive Line Enhancer," *IEEE Trans. on ASSP*, vol. ASSP-27, no. 1, pp. 31-39, Feb., 1979.
- [4] Y.H. Chang and N.J. Bershad, "Weight Modulation Effects in the Adaptive Line Enhancer," *IEEE Trans. on ASSP*, vol. ASSP-32, no. 5, pp. 1078-1081, Oct., 1984.
- [5] B. Fisher and N.J. Bershad, "ALE Behavior for two Sinusoidal Signal Models," *IEEE Trans. on ASSP*, vol. ASSP-33, no. 3, pp. 658-664, June, 1985.
- [6] R. Gooch and B. Daellenbach, "Prevention of Interference Capture in a Blind (CMA-Based) Adaptive Receive Filter," *Asilomar Conf. on Signals, Systems, Computers*, pp. 898-902, '89.
- [7] L. Li and L.B. Milstein, "Rejection of CW Interference in QPSK Systems Using Decision-Feedback Filters," *IEEE Trans. on Comm*, vol. COM-31, no. 4, pp. 473-483, April, 1983.
- [8] P. Wei, J. Zeidler, and W. Ku, "Adaptive Interference Suppression for CDMA Overlay Systems," *submitted to IEEE Journal on Selected Areas in Comm*, Sept, 1993.
- [9] C.M. Anderson, E.H. Satorius, and J.R. Zeidler, "Adaptive Enhancement of Finite Bandwidth Signals in White Gaussian Noise," *IEEE Trans. on ASSP*, vol. ASSP-31, pp. 17-28, Feb., '83.
- [10] E. Satorius, S. Krishnan, X-L Yu, L. Griffiths, I. Reed, and T-K. Trong, "Suppression of Narrowband Interference via Single Channel Adaptive Preprocessing," *Asilomar Conf. on Signals, Systems, and Computers*, pp. 270-273, 1988.
- [11] S. Haykin, *Adaptive Filter Theory* (2nd Ed.), Prentice-Hall, Englewood Cliffs, NJ, 1991.
- [12] B. Widrow, J. McCool, M. Larimore, R. Johnson, "Stationary and Nonstationary Learning Characteristics of the LMS Adaptive Filter," *Proc. IEEE*, vol. 64, pp. 1151-1162, Aug. 1976.
- [13] J.R. Glover, "Adaptive Noise Canceling Applied to Sinusoidal Interferences," *IEEE Trans. on ASSP*, vol. ASSP-25, no. 6, pp. 484-491, Dec. 1977.
- [14] M.J. Shensa, "Non-Weiner Solutions of the Adaptive Noise Canceller with a Noisy Reference," *IEEE Trans. on ASSP*, vol. ASSP-28, no. 4, pp. 468-473, Aug. 1980.
- [15] R.C. North, J.R. Zeidler, T.R. Albert, and W.H. Ku, "Comparison of Adaptive Lattice Filters to LMS Transversal Filters for Sinusoidal Cancellation," *IEEE Int. Conf. on ASSP (ICASSP)* '92, pp. 33-36, March 23-26, 1992.
- [16] B. Widrow, et. al., "Adaptive Noise Cancelling: Principles and Applications," *Proc. IEEE*, vol. 63, pp. 1692-1716, Dec. 1975.
- [17] D. Slock and T. Kailath, "Numerically Stable Fast Transversal Filters for Recursive Least Squares Adaptive Filtering," *IEEE Trans. on Signal Processing*, vol. SP-39, pp. 92-114, Jan., 1991.
- [18] R.C. North, J.R. Zeidler, T.R. Albert and W.H. Ku, "A Floating-Point Arithmetic Error Analysis of Direct and Indirect Coefficient Updating Techniques for Adaptive Lattice Filters," *IEEE Trans. on Signal Processing*, vol. SP-41, no. 5, pp. 1809-1823, May 1993.
- [19] J. Proakis, *Digital Communications* (2nd Ed.), McGraw Hill, New York, 1989.